Lagrange-multiplier-constrained optimization for designing narrowband dispersionless fiber Bragg gratings

Cheng-Ling Lee
National United University
Department of Electro-Optical Engineering
Miaoli, 360, Taiwan
E-mail: cherry@nuu.edu.tw

Ray-Kuang Lee
National Tsing-Hua University
Institute of Photonics Technologies
Hsinchu, 300, Taiwan

Yee-Mou Kao
National Changhua University of Education
Department of Physics
Changhua 500, Taiwan

Abstract. This paper presents a new synthesis method for designing complex fiber Bragg gratings (FBGs). The method is based on a multiobjective Lagrange-multiplier-constrained optimization (LMCO), to which various constraints on the designed filters can be added in consideration of practical application demands and fabrication requirements. The maximum amplitude of the index modulation profiles of the designed FBGs can be substantially reduced under constrained conditions. In contrast with the layer-peeling (LP) algorithm, the LMCO method can easily incorporate different types of requirements in terms of a user-defined cost function. Compared to stochastic approaches such as genetic algorithms, the proposed method is likewise a direct optimization method, but without using random numbers, and therefore has a smoother coupling coefficient profile as well as faster convergence. A theoretical model and investigation have been made in this study. A narrowband dispersionless FBG filter for optical fiber communication was designed, and its simulation results were compared with those of the LP algorithm. The study results demonstrate that the LMCO algorithm can provide an alternative for practical and complex fiber grating filters. [DOI: 10.1117/1.2835461]

Subject terms: dispersionless fiber Bragg gratings (FBGs); Lagrange-multiplier-constrained optimization (LMCO); grating synthesis.

Paper 070466R received May 30, 2007; revised manuscript received Aug. 21, 2007; accepted for publication Aug. 24, 2007; published online Jan. 29, 2008.

1 Introduction

Fiber Bragg gratings (FBGs) are essential optical devices both for fiber communications and for sensor applications because of their ability to act as powerful narrowband filters, optical add-drop multiplexers, dispersion compensators, and cavity mirrors in fiber lasers.[1] In this connection, the inverse design problems of designing fiber Bragg gratings have attracted many researchers in the field of fiber optics.[2–18] The complicated inverse problem amounts to finding the grating structure (amplitude only or amplitude and phase) from a specified, complex spectrum. In the literature, the layer-peeling (LP) inverse scattering method[2–9] has been widely used as a powerful tool for designing complex FBGs, especially dispersionless FBGs. By the LP method, one can find the grating structure from a given reflection spectrum simply by propagating the fields along the grating structure, while simultaneously evaluating the grating strength using a causality argument.

Although in theory dispersionless FBGs with sharp reflectivity edges and required dispersion characteristics can be inversely synthesized by using the LP algorithm, in practice there are still a number of disadvantages in designing a high-standard dispersionless FBG filter by using this method. In particular, the required grating length is typically too long for a narrowband filter, and the synthesized spatial grating profile is too complicated, with no flexibility of design. These disadvantages have severely limited the practical application of the devices. In 2003, however, an LP-based two-stage design approach was presented for designing dispersionless FBGs with shorter grating length for practical applications.[17]

In addition to the preceding methods, different Monte Carlo optimization approaches (Tabu search, genetic algorithms, and evolutionary algorithms)[15–18] have been applied to synthesize low-dispersion (linear phase) FBGs according to the mentioned specifications. In this study, a new, optimization-based approach for synthesizing narrowband dispersionless FBGs for fiber communications was investigated. The approach is based on a simple and direct algorithm, Lagrange-multiplier-constrained optimization (LMCO). The LMCO method has been proved to be very useful in designing optical pulse shapes to achieve various goals.[19–21] Recently, the LMCO optimization algorithm has been used for designing multichannel FBGs (MCFBGs) for dense wavelength-division multiplexing.[14]

In the present study, the proposed algorithm was further extended in such a way that it could handle synthesis problems involving multiobjective optimization with not only the reflection power spectrum having to be optimized but also the phase of the designed FBG filter. This is particularly important in designing narrowband dispersionless FBGs for which both the reflectivity in the whole spectrum and the in-band dispersion spectrum have to meet a required performance. In general, and in contrast with the LP algorithm, the proposed method can easily incorporate vari-

0091-3286/2008/$25.00 © 2008 SPIE

ous constraints on the designed devices for practical applications. Compared to Monte Carlo approaches, this method is a direct synthesis method that does not use random numbers and thus has a smoother coupling coefficient profile as well as faster convergence. Moreover, by varying the weighting parameters according to a user-defined cost function, the maximum index modulation of the designed gratings can be controlled to meet fabrication requirements. Therefore, in this study, the proposed algorithm also took the phase parameters of the designed filters into consideration.

The main aim of the present work has been to construct the theoretical framework and demonstrate the suitability and advantages of this method for advanced FBG filter design. In the study, a complete mathematical theory for multitarget optimal FBGs was obtained with the additional advantage of reducing the index modulation. The convergence rate was fast and direct for the LMCO algorithms compared to the stochastic approach. This is, apparently, the first demonstration that the design of dispersionless FBGs using the LMCO multitarget optimization approach can indeed be achieved.

The organization of this paper is as follows: In Sec. 2, the theoretical formulas of the LMCO algorithm for the design of dispersionless FBGs are presented. Section 3 contains numerical results and comparisons with alternative synthesis methods (for example, the layer-peeling algorithm), and finally, the main conclusions are drawn in Sec. 4. The detailed derivation of the formulations for LMCO algorithm is presented in an appendix (Sec. 5).

2 Lagrange-Multiplier-Constrained Optimization Algorithm for Designing Dispersionless FBGs

The LMCO algorithm is based on the well-known coupled-mode equations for FBGs,[1]

$$\frac{\mathrm{d}R(z)}{\mathrm{d}z} = i\delta \cdot R(Z) + i\kappa(z)S(z),$$

$$\frac{\mathrm{d}S(z)}{\mathrm{d}z} = i\delta \cdot S(Z) - i\kappa^{*}(z)R(z), \tag{1}$$

where the amplitudes R and S are the forward- and backward-mode amplitudes, $\delta = \pi(2n_0/\lambda - 1/\Lambda)$ is the wavelength detuning, and Λ is the grating period. The parameter $\kappa(z) = \xi\pi\,\Delta n(z)$ is the designed coupling-coefficient distribution function with $\Delta n(z)$ the index modulation of the gratings. The main idea of the LMCO method is to define an objective function to be minimized with respect to R and S. For the convenience of variation with respect to R and S in dispersionless FBG design, the objective function has to be defined as follows:

$$\Phi = \frac{1}{2}\int_{-\infty}^{\infty} [r(\lambda) - r_d(\lambda)]^2\,\mathrm{d}\lambda + \frac{\beta}{2}\int_{0}^{L} [\kappa(z)]^2\,\mathrm{d}z + \frac{\eta}{2}\int_{-\infty}^{\infty} r_d(\lambda)\cdot[\rho(\lambda) - \rho_d(\lambda)]^2\,\mathrm{d}\lambda, \tag{2}$$

where $r(\lambda) = |\rho(\lambda)|^2 = |S(0)/R(0)|^2$ is the reflection power spectrum, $\rho(\lambda)$ is the reflection coefficient, $\kappa(z)$ is the coupling-coefficient profile, L is the total length of the grating, and β and η are the positive numbers acting as weighting parameters for the constraint control. In Eq. (2), the deviations from the reflection power $[r(\lambda)]$ and targeted reflection power $[r_d(\lambda)]$ spectrum are integrated over all spectral points. The phase in the stop band is the only quantity that needs to be taken into consideration; the deviations from the reflection coefficient $[\rho(\lambda)]$ and the targeted reflection coefficient $[\rho_d(\lambda)]$ spectra are needed to multiply with the targeted reflection power $r_d(\lambda) = |\rho_d(\lambda)|^2$, which acts as a filter to exclude the phase spectral points outside the stop band.

In the defined objective function, Eq. (2), the spatially coupling coefficient $\kappa(z)$ was kept real and used to shape an output reflection power $r(\lambda)$ for a given reflection spectrum $r_d(\lambda)$ and to minimize the difference of reflection power spectra, the difference of in-band reflection-coefficient spectra, and the norm of the coupling-coefficient profile simultaneously.

Then the Lagrange multiplier functions were introduced:

$$\mu(\delta,z) \equiv \begin{bmatrix} \mu_R(\delta,z) \\ \mu_S(\delta,z) \end{bmatrix} \tag{3}$$

in an augmented cost functional

$$\begin{aligned} J = \Phi &+ \int_{-\infty}^{\infty} [\mu_{R,R}R_R + \mu_{R,I}R_I + \mu_{S,R}S_R + \mu_{S,I}S_I]_{-L/2}^{L/2}\mathrm{d}\lambda \\ &+ \int_{-\infty}^{\infty}\int_{-L/2}^{L/2}\left(-R_R\frac{\partial \mu_{R,R}}{\partial z} + \mu_{R,R}\delta R_I + \mu_{R,R}\kappa S_I\right)\mathrm{d}z\,\mathrm{d}\lambda \\ &+ \int_{-\infty}^{\infty}\int_{-L/2}^{L/2}\left(-R_I\frac{\partial \mu_{R,I}}{\partial z} - \mu_{R,I}\delta R_R - \mu_{R,I}\kappa S_R\right)\mathrm{d}z\,\mathrm{d}\lambda \\ &+ \int_{-\infty}^{\infty}\int_{-L/2}^{L/2}\left(-S_R\frac{\partial \mu_{S,I}}{\partial z} - \mu_{S,R}\delta S_I - \mu_{S,R}\kappa R_I\right)\mathrm{d}z\,\mathrm{d}\lambda \\ &+ \int_{-\infty}^{\infty}\int_{-L/2}^{L/2}\left(-S_I\frac{\partial \mu_{S,I}}{\partial z} + \mu_{S,I}\delta S_R + \mu_{S,I}\kappa R_R\right)\mathrm{d}z\,\mathrm{d}\lambda, \end{aligned} \tag{4}$$

where the forward and backward modes (R,S) and the Lagrange multiplier functions $\mu(\delta,z)$ were separated into real and imaginary parts: $R = R_R + iR_I$, $S = S_R + iS_I$, $\mu_R = \mu_{R,R} + i\mu_{R,I}$, and $\mu_S = \mu_{S,R} + i\mu_{S,I}$.

To minimize the cost functional J, a variational method for Eq. (4) was used with respect to the forward and backward modes through the Lagrange multipliers μ_R and μ_S. The proof is given in the appendix. The resulting equations of motion for the Lagrange multipliers are

$$\frac{\partial \mu_R(z)}{\partial z} = i\delta\mu_R(z) - i\kappa(z)\mu_S(z), \tag{5}$$

$$\frac{\partial \mu_S(z)}{\partial z} = -i\delta\mu_S(z) + i\kappa(z)\mu_R(z), \tag{6}$$

with the boundary conditions at $z=0$ given by

$$\mu_R(0) = -2r\Delta_r R(0) + \eta \cdot r_d\{\Delta_R[S(0) - 2\rho_R R(0)] - i\Delta_I[S(0) - 2\rho_I R(0)]\}, \tag{7}$$

$$\mu_s(0) = 2\Delta_r S(0) + \eta \cdot r_d R(0)\Delta, \tag{8}$$

where

$$\Delta_r = r(\lambda) - r_d(\lambda) \tag{9}$$

is the discrepancy between the output and the target reflection power, and

$$\Delta_R = \frac{\rho_R - \rho_{d,R}}{|R|^2}, \tag{10}$$

$$\Delta_I = \frac{\rho_I - \rho_{d,I}}{|R|^2} \tag{11}$$

are the real and imaginary parts of the normalized discrepancy between the complex output and target reflection coefficient spectra, respectively. Here Δ can be written as follows:

$$\Delta = \Delta_R + i\Delta_I, \tag{12}$$

where Δ is the complex discrepancy (error). Then, the cost functional J was varied again with respect to the coupling-coefficient function $\kappa(z)$:

$$\frac{\delta J}{\delta \kappa^*} = \beta \cdot \kappa + \int_{\infty}^{-\infty} (\mu_{R,R}S_I - \mu_{R,I}S_R)\, \mathrm{d}\lambda + \int_{-\infty}^{\infty} (-\mu_{S,R}R_I + \mu_{S,I}R_R)\, \mathrm{d}\lambda. \tag{13}$$

Finally, Eqs. (1)–(8) are solved in a self-consistent way with the following procedure:

(a) Guess an initial $\kappa_{\mathrm{ini}}(z)$, and let $\kappa_{\mathrm{old}}(z)=\kappa_{\mathrm{ini}}(z)$.

(b) Solve Eq. (1) to obtain $R(z)$ and $S(z)$ from $z=L$ to $z=0$.

(c) Set the boundary conditions of $\mu_R(0)$ and $\mu_S(0)$ by using Eqs. (7) and (8). Then, the propagations of the Lagrange-multiplier functions $\mu_R(z)$ and $\mu_S(z)$ from $z=0$ to $z=L$ can be obtained by solving Eqs. (5) and (6).

(d) Find $\delta J/\delta\kappa^*$ from Eq. (13) and update the new medium:

$$\kappa_{\mathrm{new}}(z) = \kappa_{\mathrm{old}}(z) - \alpha\frac{\delta J}{\delta \kappa^*}, \tag{14}$$

where α is an ad hoc constant.

(e) Repeat steps (b) to (d) until the error of discrepancy meets the criterion or the iteration number is reached.

The optimization of the LMCO method for the design of dispersionless FBGs progressed until convergence was obtained through the preceding iteration.

3 Results and Discussion

In order to evaluate the effectiveness of the proposed algorithm for the narrowband dispersionless (NBDL) FBG filter, NBDL FBGs with different parameters (length, channel spacing, and bandwidth) are presented in this section. All of the MCFBG filters were designed by using the LMCO algorithm described in the previous section with an initial Gaussian apodization profile,

$$\kappa_{\mathrm{ini}}(z) = \kappa_0 \times \left[-4\ln 2 \cdot \left(\frac{z-0.5L}{\mathrm{FWHM}}\right)^2\right] (\mathrm{mm}^{-1}), \tag{15}$$

where $\kappa_0=0.4\ \mathrm{mm}^{-1}$ is a constant, and FWHM is set to 6 mm. In the designed NBDL FBG, the target spectrum of the complex reflection coefficient for linear phase response is set to

$$\rho_d(\lambda) = \sqrt{r_0}\exp\left[-\left(\frac{\delta}{\delta_c}\right)^{10}\right]\exp(-j\times 3\pi\times\delta), \tag{16}$$

where δ (mm^{-1}) is the wavelength detuning parameter; $\delta_c=0.43\ \mathrm{mm}^{-1}$, which corresponds to a FWHM (−3-dB) bandwidth of the filter equal to about 0.2 nm, and a −0.5-dB bandwidth equal to about 0.165 nm; and r_0 is the maximum reflectivity, set to 0.99. The central wavelength was always 1550 nm. In the proposed algorithm, the units of λ and L are millimeters, and $\kappa(z)$ is in mm^{-1}.

The parameters α, β, and η are ad hoc constants, which have different roles in different designs. Here α represents the evolution of the coupling coefficient; η is a weighting phase parameter, which is nonzero for dispersionless FBGs and zero for the usual FBGs when only the reflectivity spectrum is taken into consideration; and β is a constraint parameter for the coupling coefficient of the designed fiber grating, which is zero for unconstrained conditions and nonzero for a constrained coupling coefficient. The constraint on the value of the coupling constant can be more easily enforced by sacrificing the quality of the reflectivity spectrum with an increase in the weighting parameter β. In this study, it was found that the best value of α was around 1×10^5, and of η was about 0.5, which produced optimal and smooth convergence in the designed NBDL FBG filters. The unconstrained synthesized results with $\alpha=1\times10^5$, $\eta=0.5$, and $\beta=0$ for the LMCO NBDL FBG are given below.

Figure 1 shows the synthesized reflectivity spectra of 0.2-nm NBDL FBG filters using the LMCO and LP methods. The designed reflection spectrum met well with the target spectrum for a grating length of 4 cm. The corresponding apodization profiles of the index modulation (κ)

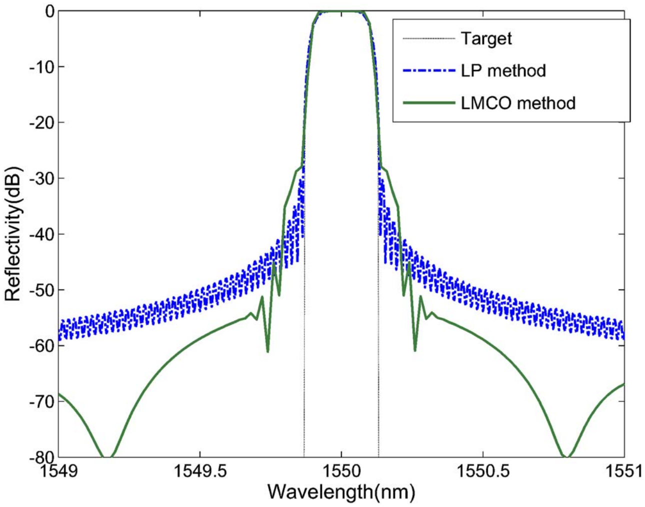

Fig. 1 The reflectivity spectra of 0.2-nm NBDL FBG filter synthesized using LMCO and LP methods.

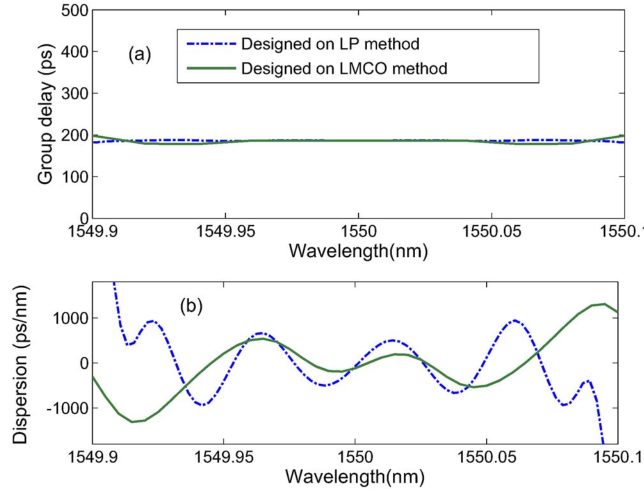

Fig. 3 The (a) in-band group delay and (b) in-band dispersion profiles of 0.2-nm NBDL-FBG filters synthesized by using LMCO and LP methods.

with the two methods are shown in Fig. 2. The results show the apodization profile of the LMCO method as being more symmetrical than with the LP method. The initial guess of the Gaussian apodization profile (dotted line) for the proposed algorithm also appears in Fig. 2 as a reference. The in-band group delay and in-band dispersion profiles of the designed NBDL FBG filters in Fig. 1 appear in Fig. 3. From Fig. 3, it can be seen that the deviation of the LMCO dispersion profile in 75% of the central region of the stop band is smoother and lower than that of the LP dispersion profile. The better synthesis result comes from the fact that we include the targeted reflection power $r_d(\lambda)$ as a factor in the third term of the cost function in Eq. (2); with this, about 75% of the central region of the stop band attains the maximum value r_0.

The comparisons for the designed reflectivity spectra, dispersion spectra, and coupling-coefficient profiles are shown in Fig. 4(a)–4(c), with different values of the parameter α. In this case, the parameter β is zero and η is 0.5. In Fig. 4(d) typical evolution curves of the calculated average error $|\Delta|$ (total error divided by the number of spectral points) for the NBDL FBG filters are shown. It is clear that the best ad hoc parameter α is about 10^5, because in this situation the average error $|\Delta|$ is the minimum. Based on our experiences, the algorithm diverges when $\alpha \geqslant 10^6$ in this designed case. As implied by Eq. (14), for a too large value of α, the modification of the coupling-coefficient profile $\kappa_{\text{new}}(z)$ at each iteration step becomes more dramatic, so that an upper bound for the ad hoc parameter α is required. On the other hand, from the results of Fig. 4(d), we see that small α is not very efficient, due to the enormous number-of iterations required when the small value $\alpha = 10^3$ is used. Basically, small α helps to find a better optimization result, but there is a trade-off between long iteration time and good optimization. In Fig. 4(b), the designed filter with lowest α (10^3) has the best dispersion profile, but the discrepancy between the designed and target reflectivity spectra of FBGs is larger than in the other cases, or else the total average error $|\Delta|$ has not reached the minimum at 1000 iterations [see Fig. 4(a) and 4(d)]. In general, the iterations typically finish after hundreds of runs (about 650 iterations) when α is about 10^5. Figure 4(d) also demonstrates that the convergence of the proposed method for NBDL FBG synthesis, involving multiobjective optimization, is efficient and effective.

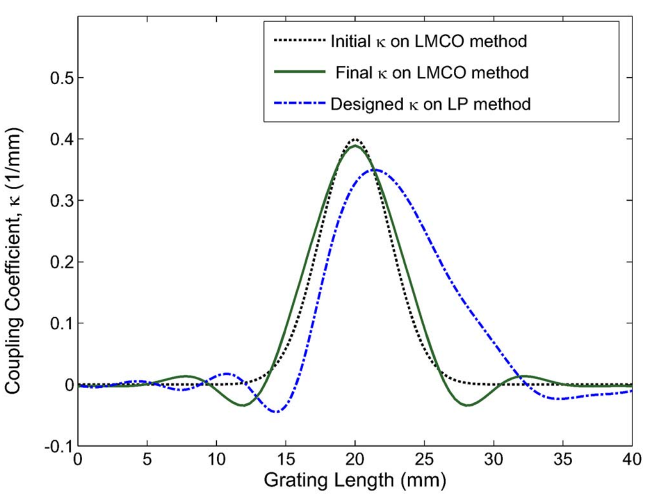

Fig. 2 The designed apodization profiles of the index modulation for 0.2-nm NBDL FBG filter synthesized by using LMCO and LP methods.

Finally, from our simulation experience, too large α will cause the algorithm to diverge, but for a lower value of α, almost the same optimization results may be achieved after more iterations if the algorithm can reach convergence. Therefore, we believe that the proposed LMCO algorithm for designing an FBG filter can converge smoothly and efficiently when a suitable value of α is used.

Furthermore, the main advantage of the proposed LMCO algorithm is easily combined, for practical application demands, with various constraint conditions on the designed devices in the defined cost functional, Eq. (2). However, in our synthesized NBDL FBG, the parameter β was

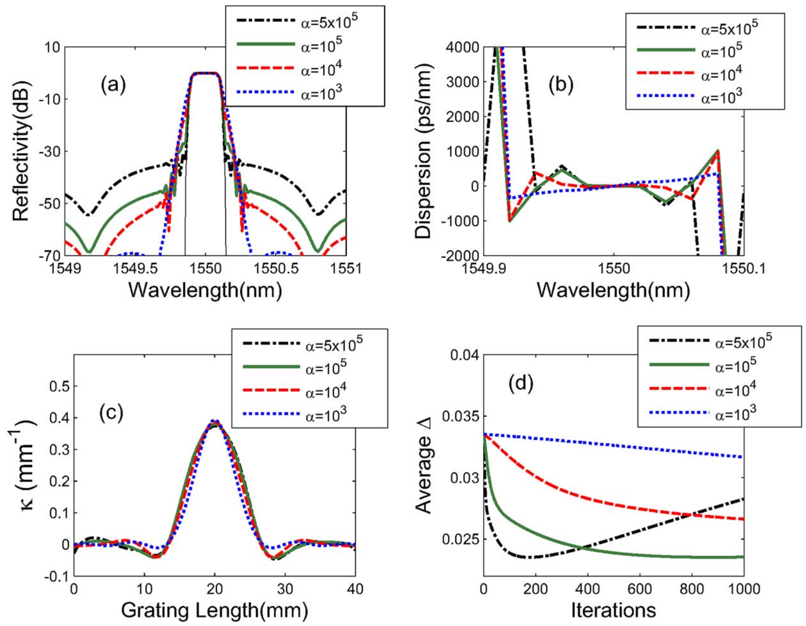

Fig. 4 The synthesized (a) reflectivity spectra, (b) in-band dispersion profiles, (c) designed apodization profiles, and (d) typical evolution curves of the average error (average $|\Delta|$) for the designed NBDL FBG filters with different α values in the LMCO method.

zero for the unconstrained coupling-coefficient profiles. By increasing β, the maximum value of the index modulation in the apodization profile can be reduced by sacrificing reflectivity of the filters with the same grating length. With the same values of $\alpha = 1 \times 10^5$ and $\eta = 0.5$ but different values of the constraint parameter β, in Fig. 5(a) we show the maximum value of the reflectivity for constrained NBDL FBG filters, and in Fig. 5(b) we show the corresponding apodization profiles of index modulation with different values of β. With only a small change of β and sacrificing a little reflectivity, the maximum value of the coupling coefficient function $\kappa(z)$ can be reduced by 25%, from 0.4 to 0.3 mm^{-1}.

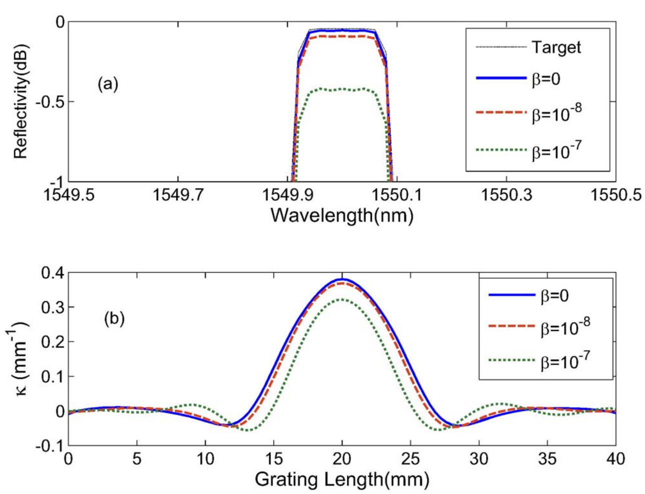

Fig. 5 The synthesized (a) reflectivity spectra (decibel scale) and (b) corresponding coupling coefficients of the designed NBDL FBG filters with different values of the constraint parameter β in the proposed method.

4 Conclusion

In conclusion, a novel NBDL FBG synthesizing method based on multiobjective Lagrange-multiplier-constrained optimization (LMCO) has been presented. The method is able to take into account multiple optimization objectives and various constrained parameters for practical application. This is especially important in NBDL FBG design, in which both the reflected power of the whole spectrum and the phase response of the in-band spectrum must be simultaneously optimized. In contrast with stochastic approaches such as genetic algorithms, the proposed method is a direct optimization method (with sectional structure) that does not use random numbers and therefore has a smoother coupling-coefficient profile as well as faster convergence. Comparing it with the existing results from the powerful layer-peeling (LP) method, we have demonstrated that an optimal 25-GHz (0.2-nm) NBDL FBG with an adaptive design for multiobjective optimization can be obtained by using the proposed method.

Finally, except for the longer computation time, a number of advantages in using the proposed LMCO approach for solving the inverse design problems of FBGs have been identified. These advantages include the possibility of constraining the patterns of the coupling-coefficient profiles, of constraining the fiber grating length, and of obtaining better solutions by suitably arranging the weighting parameters with regard to cost. These features certainly have great merits in designing practical fiber grating devices with special requirements.

Acknowledgments

The authors thank Prof. Yinchieh Lai for useful discussions. This research is supported by the National Science Council of the Republic of China, NSC 95-2221-E-239-053 and NSC 95-2120-M-001-006.

Appendix

In this appendix, we give the detailed derivations of the equations of motion for the Lagrange multipliers in Eqs. (5) and (6) and the boundary condition for the Lagrange multipliers in Eqs. (7) and (8). First of all, we minimize the cost functional J in Eq. (4) by the variational method. By variation of Eq. (4) with respect to R_R and R_I, we get

$$-\frac{\partial \mu_{R,R}}{\partial z} - \mu_{R,I}\sigma + \mu_{S,I}\kappa = 0, \tag{17a}$$

$$-\frac{\partial \mu_{R,J}}{\partial z} + \mu_{R,R}\sigma - \mu_{S,R}\kappa = 0. \tag{17b}$$

Varying with respect to R_R and R_I again, the following equations are obtained:

$$-\frac{\partial \mu_{S,R}}{\partial z} + \mu_{S,I}\sigma - \mu_{R,I}\kappa = 0, \tag{18a}$$

$$\frac{\partial \mu_{S,I}}{\partial z} - \mu_{S,R}\sigma + \mu_{R,R}\kappa = 0. \tag{18b}$$

For $\mu_R = \mu_{R,R} + i\mu_{R,I}$ and $\mu_S = \mu_{S,R} + i\mu_{S,I}$, the resulting equations of motion for the Lagrange multipliers (17) and (18) can be rearranged as Eqs. (5) and (6) in Sec. 2.

The boundary conditions for $R(L)$ and $S(L)$ are determined by the initial conditions. The boundary conditions for the Lagrange multipliers μ_R, μ_S can be obtained by variation with respect to R and S at $z=0$ [i.e., $\partial J/\partial R_R(0), \partial J/\partial R_I(0), \partial J/\partial S_R(0), \partial J/\partial S_I(0)$], and finally the required boundary conditions are

$$\mu_{R,R}(0) = -2R_R r\Delta_r + \eta r_d[\Delta_R(S_R - 2\rho_R R_R) + \Delta_I(S_I - 2\rho_I R_R)], \tag{19a}$$

$$\mu_{R,I}(0) = -2R_I r\Delta_r + \eta r_d[\Delta_R(S_I - 2\rho_R R_I) + \Delta_I(-S_R - 2\rho_I R_I)], \tag{19b}$$

$$\mu_{S,R}(0) = 2S_R\Delta_r + \eta r_d[\Delta_R R_R - \Delta_I R_I)], \tag{19c}$$

$$\mu_{S,I}(0) = 2S_I\Delta_r + \eta r_d[\Delta_R R_I + \Delta_I R_R)], \tag{19d}$$

where $\Delta_r = r(\lambda) - r_d(\lambda)$, $\Delta_R = (\rho_R - \rho_{d,R})/|R|^2$, $\Delta_I = (\rho_I - \rho_{d,I})/|R|^2$, $\Delta = \Delta_R + i\Delta_I$, and η is an ad hoc positive constant.

Equations (19a)–(19d) are rearranged with $\mu_R(0) = \mu_{R,R}(0) + i\mu_{R,I}(0)$ and $\mu_S(0) = \mu_{S,R}(0) + i\mu_{S,I}(0)$ to obtain Eqs. (7) and (8), which are the boundary conditions for the Lagrange multipliers μ_R, μ_S at $z=0$.

References

1. T. Erdogan, "Fiber grating spectra," *J. Lightwave Technol.* **15**(8), 1277–1294 (1997).
2. A. M. Bruckstein and T. Kailath, "Inverse scattering for discrete transmission-line models," *SIAM Rev.* **29**(3), 359–389 (1987).
3. A. M. Bruckstein, B. C. Levy, and T. Kailath, "Differential methods in inverse scattering," *SIAM J. Appl. Math.* **45**(2), 312–335 (1985).
4. E. Brinkmeyer, "Simple algorithm for reconstructing fiber gratings from reflectometric data," *Opt. Lett.* **20**(8), 810–812 (1995).
5. E. Peral, J. Capmany, and J. Marti, "Iterative solution to the Gel'fand-Levitan-Marchenko coupled equations and application to the synthesis of fiber gratings," *IEEE J. Quantum Electron.* **32**(12), 2078–2084 (1996).
6. M. A. Muriel, J. Azana, and A. Carballar, "Fiber grating synthesis by use of time-frequency representations," *Opt. Lett.* **23**(19), 1526–1528 (1998).
7. R. Feced, M. N. Zervas, and M. A. Muriel, "An efficient inverse scattering algorithm for the design of nonuniform fiber Bragg gratings," *IEEE J. Quantum Electron.* **35**(8), 1105–1115 (1999).
8. L. Poladian, "Simple grating synthesis algorithm," *Opt. Lett.* **25**, 787–789 (2000).
9. J. Skaar, L. Wang, and T. Erdogen, "On the synthesis of fiber Bragg grating by layer peeling," *IEEE J. Quantum Electron.* **37**(2), 165–173 (2001).
10. J. Skaar and K. M. Risvik, "A genetic algorithm for the inverse problem in synthesis of fiber gratings," *J. Lightwave Technol.* **16**(10), 1928–1932 (1998).
11. C.-L. Lee and Y. Lai, "Evolutionary programming synthesis of optimal long-period fiber grating filters for EDFA gain flattening," *IEEE Photonics Technol. Lett.* **14**(11), 1557–1559 (2002).
12. C.-L. Lee, "Designing optimal long-period fiber gratings with the overlapped Gaussian-apodization method for flattening EDFA gain spectra," *Opt. Commun.* **262**, 170–174 (2006).
13. S. Baskar, P. N. Suganthan, N. Q. Ngo, A. Alphones, and R. T. Zheng, "Design of triangular FBG filter for sensor applications using covariance matrix adapted evolution algorithm," *Opt. Commun.* **260**, 716–722 (2006).
14. C.-L. Lee, R.-K. Lee, and Y.-M. Kao, "Design of multichannel DWDM fiber Bragg grating filters by Lagrange multiplier constrained optimization," *Opt. Express* **14**(23), 11002–11011 (2006).
15. S. Baskar, R. T. Zheng, A. Alphones, N. Q. Ngo, and P. N. Suganthan, "Particle swarm optimization for the design of low-dispersion fiber Bragg gratings," *IEEE Photonics Technol. Lett.* **17**(3), 615–617 (2005).
16. C.-L. Lee and Y. Lai, "Optimal narrowband dispersionless fiber Bragg grating filters with short grating length and smooth dispersion profile," *Opt. Commun.* **235**, 99–106 (2004).
17. J. Skaar and K. M. Risvik, "Design and characterization of finite length fiber gratings," *IEEE J. Quantum Electron.* **39**(10), 1238–1245 (2003).
18. N. Q. Ngo 1, R. T. Zheng, S. C. Tjin, and S. Y. Li, "Tabu search synthesis of cascaded fiber Bragg gratings for linear phase filters," *Opt. Commun.* **241**, 79–85 (2004).
19. N. Wang and H. Rabitz, "Optimal control of pulse amplification without inversion," *Phys. Rev. A* **53**(3), 1879–1885 (1996).
20. N. Wang and H. Rabitz, "Optimal control of population transfer in an optical dense medium," *J. Chem. Phys.* **104**(4), 1173–1178 (1996).
21. R. Buffa, "Optimal control of population transfer through the continuum," *Opt. Commun.* **153**, 240–244 (1998).

Cheng-Ling Lee received her MS. degree from the Institute of Electro-Optical Engineering, National Chiao Tung University (IEO/NCTU), Taiwan, in 1991. After several years working as a teacher as well as a research student, she obtained her PhD degree from the IEO/NCTU in 2003. She is now a researcher and an associate professor with the Department of Electro Optical Engineering, National United University, Taiwan. Her special fields of interest include fiber grating synthesis, fiber-based devices, optical thin-film coatings and optimization algorithms.

Ray-Kuang Lee received his BS degree from the Department of Electrical Engineering of National Taiwan University (EE/NTU) in 1993, and his MS degree and PhD degree from the Institute of Electro-Optical Engineering of National Chiao Tung University (IEO/NCTU), in 1999 and 2004, respectively. He worked as an assistant scientist at the National Center for High-Performance Computing, Taiwan, from 2001 to 2004, and as a visiting fellow at The Australian National University, Australia, in 2004. Then he joined the Institute of Photonics Technologies of National Tsing Hua University as a faculty member in August 2005. He is currently an assistant professor at the Institute of Photonics Technologies. His research interests include nonlinear optics, quantum optics, and device synthesis.

Yee-Mou Kao received his MS and PhD degrees in physics from National Tsing Hua University, Hsinchu, Taiwan, in 1991 and 1996, respectively. Currently he is an associate professor in the Department of Physics, National Changhua University of Education, Changhua, Taiwan. His research interests are mainly on the statistical physics related problems. Recently, he has been engaged in the study of thermodynamic properties of trapped Bose-Einstein condensates.